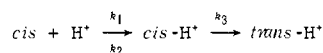


- 3907 (1968); (b) E. Fischer and V. F. Frei, *J. Chem. Phys.*, **27**, 328 (1957).
- (17) Amino and hydroxy substituted dyes, however, show large solvent effects on the positions of the  $\pi$ - $\pi^*$  maxima; see W. R. Brode, J. H. Gould, and G. M. Wyman, *J. Amer. Chem. Soc.*, **74**, 4641 (1952).
- (18) N. C. Baird, P. De Mayo, J. R. Swenson, and M. C. Usselman, *J. Chem. Soc., Chem. Commun.*, **9**, 314 (1973).
- (19) Comparison of rate constants (extrapolated from data of ref 16a) of this compound with those of other methyl-substituted azobenzenes<sup>1d,2f</sup> shows the hexamethylazobenzene to isomerize slower by two powers of 10.
- (20) From the steady state approximation for cis H<sup>+</sup> for the reaction sequence:



in which  $k_H[H^+]$  is  $k_1 k_3 [H^+] / (k_2 + k_3)$ . The first-order rate constant describes the process  $cis \rightarrow trans$  ( $k_s$ ) in the aqueous system.

- (21) Determined by application of the Arrhenius equation to the value of the slopes of plots at 30.2 and 20.0°.
- (22) S. Ljunggren and G. Wettermark, *Acta Chem. Scand.*, **25**, 1599 (1971).
- (23) The dihedral angles (designated  $\phi = \phi_1, \phi_2$ ) specify the angle described by the nodal plane of the azo  $\pi$ -system nodal planes. For the planar molecule,  $\phi = 0, 0^\circ$ , and for the  $n$ - $\pi$  aligned molecule,  $\phi = 90, 90^\circ$ .
- (24) (a) J. M. Robertson, *J. Chem. Soc.*, 232 (1939); (b) A. Mostad and C. Romming, *Acta Chem. Scand.*, **25**, 3561 (1971).
- (25) H. Suzuki, "Electronic Absorption Spectra and Geometry of Organic Molecules," Academic Press, New York, N.Y., 1967.
- (26) B. Kellerer, H. H. Hacker, and J. Brandmuller, *Indian J. Pure Appl. Phys.*, **9**, 903 (1971).
- (27) (a) V. A. Ismailski and E. A. Smirnov, *Zh. Obshch. Khim.*, **26**, 3389 (1956); (b) N. Ebara, *Bull. Chem. Soc. Jap.*, **33**, 534 (1960); (c) W. F. Smith, *Tetrahedron*, **19**, 445 (1963); (d) E. Haselbach and E. Heilbronner, *Helv. Chem. Acta*, **51**, 16 (1968).
- (28) CNDO/2 calculations were performed with the program described by J. A. Pople and D. L. Beveridge, "Approximate Molecular Orbital Theory," McGraw-Hill, New York, N.Y., 1970.
- (29) B. Bak, L. Hansen-Nygaard, and J. Rastrup-Andersen, *J. Mol. Spectrosc.*, **2**, 361 (1968).
- (30) With  $\phi = 45, 45^\circ$ , the ring planes are each twisted 45° like the blades of a propeller with respect to the nodal plane of the azo  $\pi$  system.
- (31) D. J. W. Bullock, C. W. N. Cumper, and A. I. Vogel, *J. Chem. Soc.*, 5316 (1965).
- (32) J. Kroner and H. Bock, *Chem. Ber.*, **101**, 1922 (1968).
- (33) Energies calculated with NN = 1.23 Å; CH = 1.41, 1.41 Å;  $\phi = 121, 121$ .  $\pi$ - $\pi$ ,  $\pi$ - $\pi$  alignment refers to the alignment of the azo  $p$ - $\pi$  orbitals with the adjacent ring  $\pi$  systems.
- (34) (a) G. Wettermark and L. Bogliotti, *J. Chem. Phys.*, **40**, 1486 (1964); (b) G. Wettermark, J. Weinstein, J. Sousa, and L. Bogliotti, *ibid.*, **40**, 1486 (1964); (c) C. H. Warren, G. Wettermark, and K. Weiss, *J. Amer. Chem. Soc.*, **93**, 4658 (1971).
- (35) To our knowledge, mention of the two possible routes was apparently first made in a reference in the article of D. Y. Curtin and J. Hauser, *J. Amer. Chem. Soc.*, **88**, 2775 (1966).
- (36) The estimate of the curvature in the Arrhenius plots was obtained by calculating  $E_a$  by the Arrhenius expression from points at 20 and 25°, and at 60 and 65°.
- (37) K. J. Ladler, "Chemical Kinetics," McGraw-Hill, New York, N.Y., 1965, pp 198-253.
- (38) J. H. Bowie and G. E. Lewis, *J. Chem. Soc. B*, 621 (1967).
- (39) This can be seen by inspection of the data presented in ref 2f.
- (40) (a) G. E. Hall, W. J. Middleton, and D. D. Roberts, *J. Amer. Chem. Soc.*, **93**, 4778 (1971); (b) W. G. Herkstroeter, *J. Amer. Chem. Soc.*, **95**, 8686 (1973).

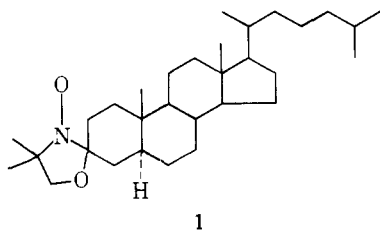
## Assignment of the Configuration of the Steroid Spin Label, 3-Doxyl-5 $\alpha$ -cholestane

Thomas B. Marriott, G. Bruce Birrell, and O. Hayes Griffith\*

Contribution from the Department of Chemistry and the Institute of Molecular Biology, University of Oregon, Eugene, Oregon 97403. Received July 26, 1974

**Abstract:** There are two possible isomers of the useful steroid spin label, 3-doxyl-5 $\alpha$ -cholestane [CA 18353-76-9]. In order to determine which of these isomers is present in the recrystallized synthetic product, the spin label was trapped in a thiourea inclusion crystal. An esr spectral analysis unambiguously identifies the included spin label as 3(e)-doxyl-5 $\alpha$ -cholestane, the isomer with the C-N bond in the equatorial position with respect to the steroid A ring. By computer subtraction of the corresponding solution spectrum, it is estimated that at least 95% of the recrystallized synthetic product is the equatorial isomer. No axial isomer was detected in the recrystallized synthetic product or the inclusion crystals.

In 1967 Keana, Keana, and Beetham<sup>1</sup> introduced what has become one of the widely used spin labels for studying biological membranes. The molecule is 3-doxyl-5 $\alpha$ -cholestane (**1**), the 4',4'-dimethyloxazolidine-*N*-oxyl derivative of 5 $\alpha$ -cholestan-3-one.



Important information concerning the orientation, anisotropic motion, and diffusion of membrane lipids is being obtained using this steroid and closely related derivatives.<sup>2-8</sup> An analysis of the resulting electron spin resonance line shapes requires a knowledge of the stereochemistry of **1**. Given the stereochemistry of the parent compound, 5 $\alpha$ -cholestan-3-one, the oxazolidine ring formation leads to two possible isomers as shown in Figure 1. The purpose of this study is to identify which of these two isomers predominates

in the crystalline product used in the spin-labeling experiments.

We approach this problem by trapping **1** in the tubular cavities of a thiourea inclusion crystal. The basic structure of the thiourea inclusion crystal, which is independent of the guest molecule, has hexagonal cavities 7 Å in diameter extending along the sixfold symmetry axis. The guest molecule **1** can only orient in the tubular cavities with its long axis ( $z_2$ ) parallel to the needle axis of the crystal. With this knowledge of the orientation and an analysis of the esr spectral anisotropy, it is possible to unambiguously identify the isomer of **1** present in the crystal.

### Experimental Section

3-Doxyl-5 $\alpha$ -cholestane was synthesized from 5 $\alpha$ -cholestan-3-one (Steraloids, Inc.) by the procedure of Keana, *et al.*,<sup>1</sup> and recrystallized from ethanol (mp 160-161° uncor). Single crystals of the 3-doxyl-5 $\alpha$ -cholestan-3-one-thiourea inclusion compound were grown as follows. The spin label (8 mg) was dissolved in 6 ml of ethanol saturated with thiourea (Mallinckrodt); this solution was saturated with D(+)-camphor (U. S. P. grade, Aldrich Chemical Co.); a small excess of camphor was then added and the solution warmed on a hot plate to dissolve the excess; the warmed solution was al-

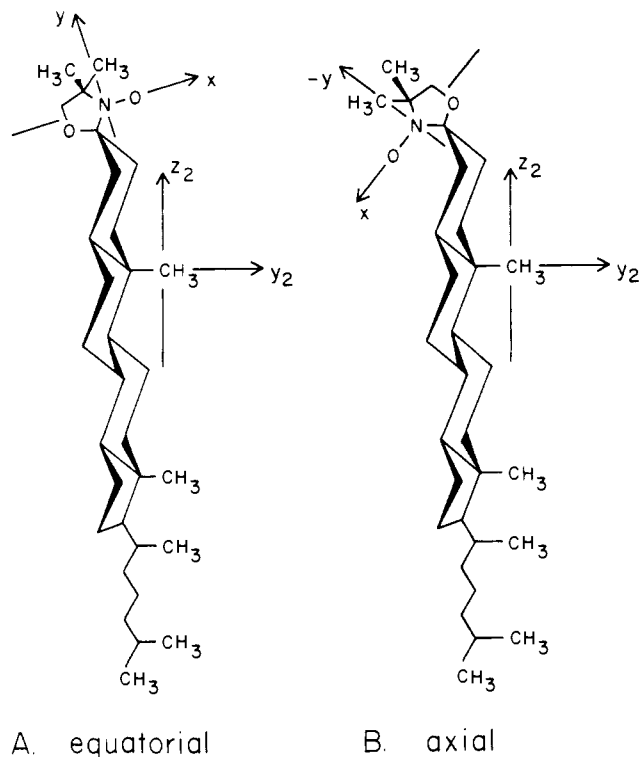


**Figure 1.** Structures of the two isomers of the 3-doxyl-5 $\alpha$ -cholestane spin label.

lowed to cool to room temperature with small needle-like crystals forming over a period of 3 hr. The camphor acts as a molecular spacer to minimize magnetic interactions between spin labels in the tubular cavities of the inclusion crystal.

The esr spectra of several inclusion crystals (1  $\times$  3 mm) aligned on the Teflon tip of a crystal mount were recorded at 9.5 GHz on a Varian E-line spectrometer.  $A$  and  $g$  values were measured using a V-4502 spectrometer equipped with a V-4532 dual cavity. The  $A$  values were measured as the distance between the low-field and center lines on the single-crystal esr spectra (because of line broadening of the high-field line at some orientations). Di-*tert*-butyl nitroxide was used as a reference. A  $5 \times 10^{-4}$   $M$  solution of this nitroxide in 0.01  $M$  phosphate buffer (pH 7.0) has an  $^{14}\text{N}$  coupling constant of  $17.16 \pm 0.01$  G and a  $g$  value of  $2.0056 \pm 0.0001$ .<sup>9</sup>

The solution spectrum of 3-doxyl-5 $\alpha$ -cholestane, which had previously been trapped in inclusion crystals, was obtained in the following manner. The inclusion crystal (17.3 mg) was dissolved in 1.3 ml of  $\text{H}_2\text{O}$ -methanol (3:1, v/v) and then extracted with 1.0 ml of  $\text{CDCl}_3$ . The  $\text{CDCl}_3$  solution was deoxygenated by bubbling  $\text{N}_2$  into it. Solution spectra were recorded at 9.5 GHz on a Varian E-line spectrometer with the modulation amplitude set at  $2 \times 10^{-2}$  G.

## Results and Discussion

**A. General Properties of the Inclusion Crystals and Orientation of the Guest Molecules.** ESR spectra of the cholestane nitroxide trapped in thiourea consist of  $2I + 1 = 3$  lines with the center position ( $g$  value) and  $^{14}\text{N}$  hyperfine splitting ( $A$ ) varying with the orientation of the crystal in the magnetic field ( $H$ ). Defining  $Z_1$  to be the needle axis of the inclusion crystal, the esr spectra with  $H$  parallel and perpendicular to this axis are shown in Figure 2. These spectra represent the minimum and maximum splittings observed for any orientation of the crystal and are therefore the principal orientations. The  $H$  perpendicular to  $Z_1$  spectrum is invariant to rotation of the crystal about its needle axis. This interesting behavior, combined with the observed line shape, can result only from rapid rotation or large amplitude oscillations of the spin label about the *crystalline*  $Z_1$  axis and is consistent with previous studies showing that or-

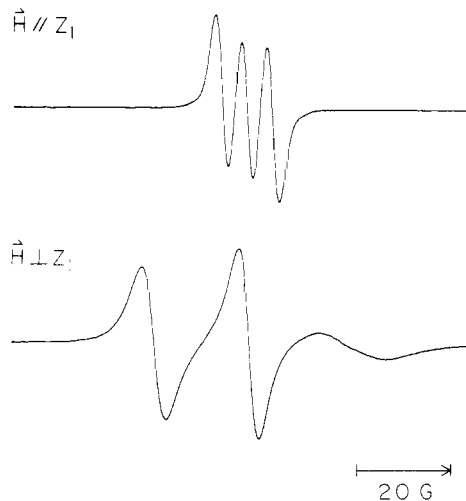


**Figure 2.** Room temperature esr spectra of 3-doxyl-5 $\alpha$ -cholestane trapped in a single crystal of thiourea. The top and bottom spectra were recorded with the magnetic field parallel and perpendicular to the crystalline needle axis,  $Z_1$ , respectively.

ganic molecules trapped in thiourea exhibit a high degree of motion.<sup>9-13</sup>

A molecular model of the hexagonal cavity in the thiourea inclusion crystal was constructed using the X-ray crystallographic data of Lenne<sup>11</sup> and Schlenk<sup>12</sup> (Figure 3). This cavity parallels the crystalline needle axis,  $Z_1$ . Corey-Pauling-Koltun space-filling models of both isomers of the cholestane nitroxide are essentially cylindrical in shape with a length of 24  $\text{\AA}$  (along the  $z_2$  molecular axis) and a diameter of 6  $\text{\AA}$ . Upon inclusion, either isomer would be oriented with the molecular  $z_2$  axis parallel to the crystalline needle axis,  $Z_1$  (Figure 4). The invariance of the esr spectrum to rotation about  $Z_1$  when  $H$  is perpendicular to  $Z_1$  can now clearly be interpreted as the result of rapid rotation or large amplitude oscillation about the *molecular* axis,  $z_2$ .

**B. The Anisotropy of the ESR Spectra Fits Only the Equatorial Isomer.** An esr spectral determination of orientation or molecular motion requires a knowledge of the spatial relationship between the nitroxide axes ( $x, y, z$ ) and the molecular axes ( $x_2, y_2, z_2$ ) of both the cholestane nitroxide isomers in Figure 1. The 3(e)-doxyl-5 $\alpha$ -cholestane (isomer A) has the N-O group in an equatorial position on the same side of the steroid A ring as the  $\text{C}_{19}$  axial methyl group and has been referred to as the *cis* isomer.<sup>3</sup> Isomer B, 3(a)-doxyl-5 $\alpha$ -cholestane, has the N-O group in an axial position. The nitroxide  $z$  axis, defined as parallel to the nitrogen and oxygen 2p orbitals associated with the unpaired electron, is nearly perpendicular to the long molecular  $z_2$  axis in both isomers. However, the orientation of the nitroxide  $y$  axis differs with respect to the  $z_2$  axis in the two cases. Previous studies employing the cholestane nitroxide spin label<sup>2-8</sup> acknowledge the possible existence of both isomers but assume the presence of only the equatorial isomer, 3(e)-doxyl-5 $\alpha$ -cholestane, for the purpose of theoretical treatments. Inclusion of the cholestane nitroxide in thiourea affords the opportunity of using esr spectral anisotropy to examine this assumption.

The rapid rotation model provides a good description of the spectral anisotropy of this spin label trapped in thiourea in spite of the fact that the relative line heights of the  $H$  perpendicular to  $Z_1$  spectrum in Figure 2 indicate that we are dealing with a somewhat lower frequency or amplitude of motion. The rapid rotation model is justified because the  $H$  perpendicular to the  $Z_1$  spectrum is isotropic to rotation about  $Z_1$  and because we are more interested in  $A$  and  $g$  value anisotropy than spectral line shape. Detailed descrip-

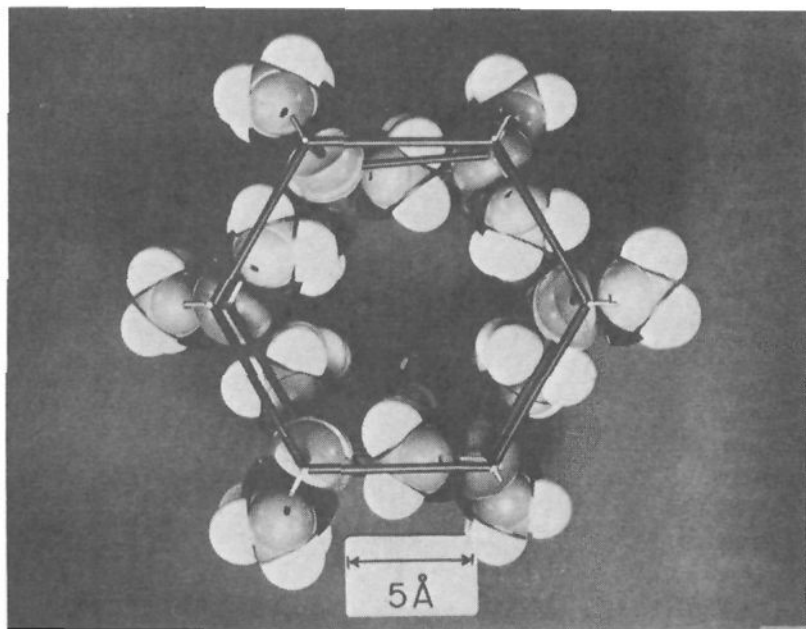


**Figure 3.** Top view of the hexagonal cavity formed in thiourea crystals. The diameter of the cavity is approximately 7 Å.

tions of the rapid rotation model for spin labels are given elsewhere.<sup>4,14</sup> The main effect of rapid rotation is to reduce the spin Hamiltonian to an axially symmetric form with motion-averaged principal values  $\bar{g}_{\parallel}$ ,  $\bar{g}_{\perp}$ , and  $\bar{A}_{\parallel}$ ,  $\bar{A}_{\perp}$ . For example

$$\bar{g}_{\parallel} = g_{zz} \cos^2 \theta_2 + g_{yy}(1 - \cos^2 \theta_2) + (g_{xx} - g_{yy}) \sin^2 \theta_2 \cos^2 \psi_2 \quad (1)$$

and

$$\bar{g}_{\perp} = g_{zz}^{1/2}(1 - \cos^2 \theta_2) + g_{yy}(1 + \cos^2 \theta_2) + (g_{xx} - g_{yy})^{1/2}(1 - \sin^2 \theta_2 \cos^2 \psi_2) \quad (2)$$

where  $g_{xx}$ ,  $g_{yy}$ ,  $g_{zz}$  are the principal values of the nitroxide  $g$  tensor.  $\cos \theta_2$  is the direction cosine between the molecular  $z_2$  axis and the nitroxide  $z$  axis and  $\cos \psi_2$  is the direction cosine between  $y_2$  and  $y$  (see Figure 1). The corresponding equations for  $\bar{A}_{\parallel}$  and  $\bar{A}_{\perp}$  are exactly the same as eq 1 and 2 with  $A_{xx}$ ,  $A_{yy}$ ,  $A_{zz}$  replacing  $g_{xx}$ ,  $g_{yy}$ ,  $g_{zz}$ . The resulting anisotropy equations are

$$g = \bar{g}_{\parallel} \cos^2 \theta_0 + \bar{g}_{\perp} \sin^2 \theta_0 \quad (3)$$

and

$$A = (\bar{A}_{\parallel}^2 \cos^2 \theta_0 + \bar{A}_{\perp}^2 \sin^2 \theta_0)^{1/2} \quad (4)$$

where  $\theta_0$  is the angle between the magnetic field and the axis of rotation,  $z_2$ ; and  $g$  and  $A$  characterize the three-line esr spectrum in the laboratory coordinates.

We now calculate the motion averaged  $A$  and  $g$  principal values from eq 1 and 2. From Figure 1 it is evident that the  $z_2$  molecular axis lies in the  $xy$  plane of the nitroxide and the molecular  $x_2$  axis is parallel to the nitroxide  $z$  axis for both isomers. Thus  $\theta_2$ , defined by the direction cosine between  $z_2$  and  $z$ , is  $\sim 90^\circ$  in each case. However,  $\psi_2$ , defined by the direction cosine between  $y_2$  and  $y$ , differs considerably for the two isomers, being approximately  $106^\circ$  for the equatorial isomer and  $-35^\circ$  for the axial isomer. Using these values of  $\theta_2$  and  $\psi_2$  and the principal values of 2-dox-

**Table I.** Calculated and Experimental Motion Averaged Principal Values

	Equatorial isomer	Axial isomer	Exptl <sup>a</sup>
$\bar{g}_{\parallel}$	2.0060	2.0078	2.0061
$\bar{g}_{\perp}$	2.0054	2.0045	2.0055
$\bar{A}_{\parallel}$ , G	5.4	5.7	5.5
$\bar{A}_{\perp}$ , G	19.4	19.2	20.0

<sup>a</sup> The experimental errors are estimated to be  $\pm 0.0002$  for  $g$  and  $\pm 0.1$  for  $A$ .

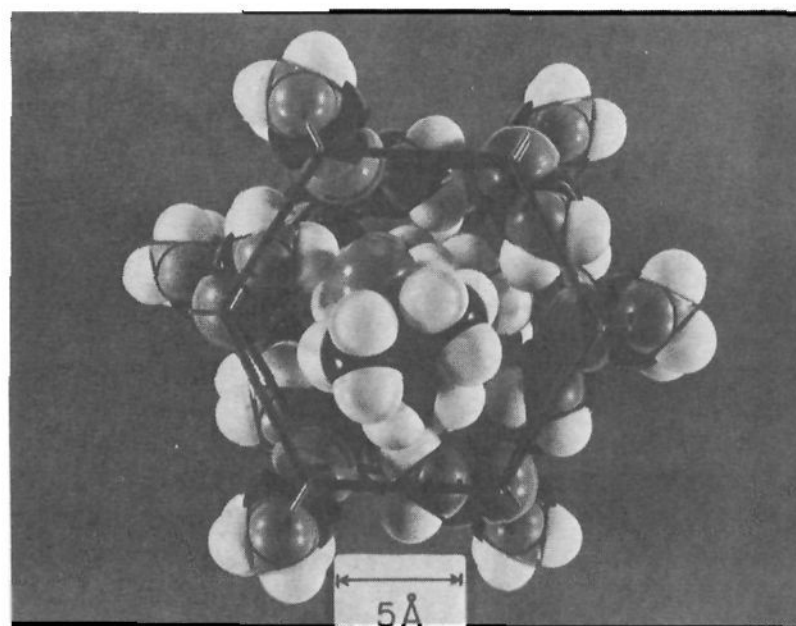


**Figure 4.** Top view of the hexagonal cavity in a thiourea inclusion crystal occupied by the 3(e)-doxyl-5 $\alpha$ -cholestane molecule.

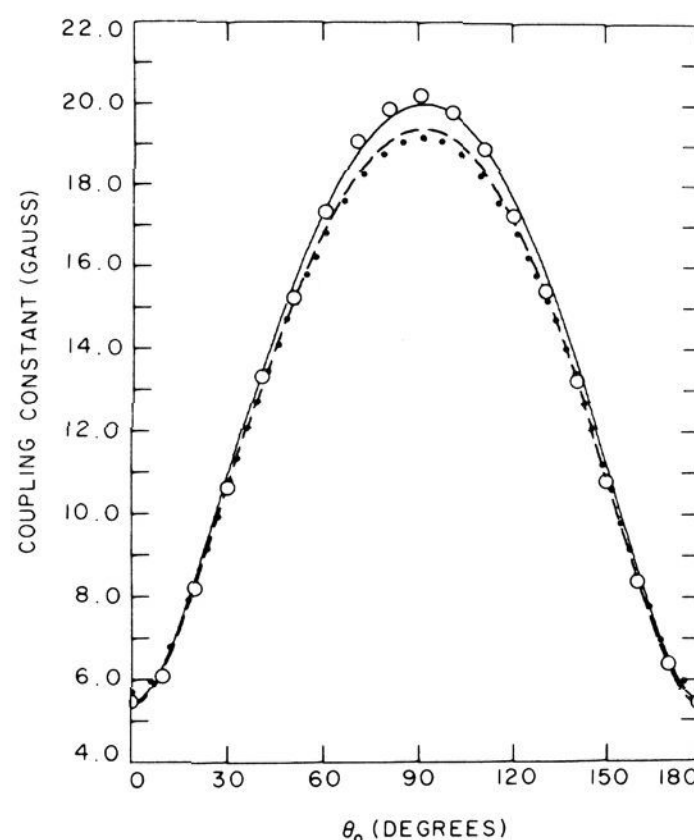


**Figure 5.** Anisotropy of the splitting constant of 3-doxyl-5 $\alpha$ -cholestane trapped in thiourea. The open circles are experimental points. The dashed and dotted lines are the predicted anisotropies of the equatorial and axial isomers, respectively.

ylpropane ( $g_{xx} = 2.0088$ ,  $g_{yy} = 2.0058$ ,  $g_{zz} = 2.0022$ ,  $A_{xx} = 5.9$  G,  $A_{yy} = 5.4$  G,  $A_{zz} = 32.9$  G)<sup>15</sup> in eq 1 and 2, the motion averaged principal values for each isomer are those given in the first two columns of Table I. There is little difference between  $\bar{A}_{\parallel}$  or  $\bar{A}_{\perp}$  calculated for the two isomers. However, significant differences exist in the averaged  $g$  values of the equatorial and axial isomers. The  $g$  value anisotropy described by eq 3 thus affords a means of distinguishing between the two isomers.

Esr spectra of the cholestane nitroxide in a thiourea inclusion crystal were recorded at  $10^\circ$  intervals from  $0$  to  $180^\circ$  as the crystal was rotated in the magnetic field. Since the cholestane nitroxide is oriented in the inclusion crystal with the molecular  $z_2$  axis coincident with the  $Z_1$  axis,  $\theta_0$  in eq 3 and 4 becomes the angle between the magnetic field and the  $Z_1$  crystal axis. In Figure 5 the experimental splittings and the predicted splittings for each isomer calculated from eq 4 are plotted vs.  $\theta_0$ . This plot does not clearly determine which isomer is included but the similarity of the predicted and experimental curves supports the use of the rotation model to describe the overall experiment.

A plot of the experimental  $g$  values vs.  $\theta_0$  is given in Fig-

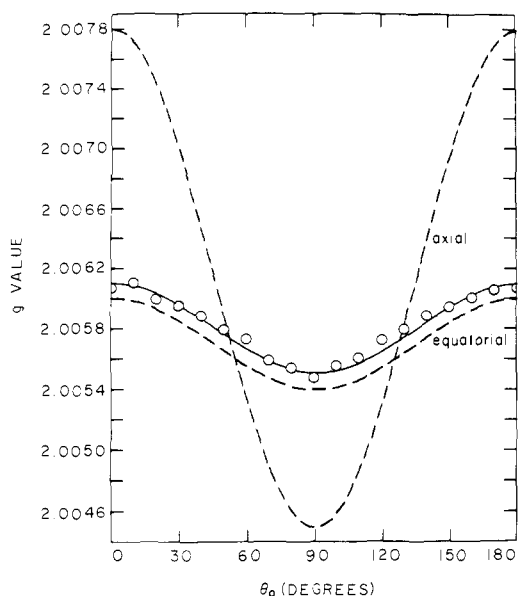


**Figure 6.** The  $g$  value anisotropy of 3-doxyl-5 $\alpha$ -cholestane included in the thiourea host crystal. The open circles are experimental points. The dashed lines are the predicted anisotropies of the equatorial and axial isomers.

ure 6. Also plotted in Figure 6 are the predicted  $g$  value anisotropies for the equatorial and axial isomers calculated from eq 3 and the motion averaged principal values of Table I. We note that the experimental curve (solid line) is very nearly the same as that predicted for the equatorial isomer. The difference between these two curves can be accounted for by the choice of the 2-doxylpropane values and polarity effects. The predicted anisotropy curve of the axial isomer is markedly different from the experimental data. No spectral lines are observed which could be assigned to the axial isomer. The presence of as little as 10% of the axial isomer would have easily been detected because of the large difference in  $g$  value anisotropies. We conclude therefore that only the equatorial isomer, 3(e)-doxyl-5 $\alpha$ -cholestane, is present in the thiourea inclusion crystal.

**C. Solution Spectra Confirm That the Equatorial Isomer Predominates in the Synthetic Product.** Thus far we have shown that only the equatorial isomer is detected in the inclusion crystal. The next logical step is to conclude that only the equatorial isomer is present in the recrystallized product from the 3-doxyl-5 $\alpha$ -cholestane synthesis. There is, however, a possibility that the inclusion crystal preferentially selects the equatorial isomer from the synthetic product. For example, it has been reported that when thiourea inclusion crystals are formed from mixtures of squalene isomers the all-trans isomer is preferentially included.<sup>13</sup> The models of Figure 1 show that the N-O and 4'-methyl groups of the axial isomer distort the cylindrical symmetry which could make it thermodynamically less likely to be trapped in the inclusion crystals. In order to examine this possibility the solution spectra of the trapped spin label and that of the crystalline reaction product are compared. These solution spectra are given in Figure 7. There is no discernible difference between these two spectra. Furthermore, we have performed a spectral subtraction of spectrum a from b and find no residual component.<sup>16</sup> We conclude that the overwhelm-

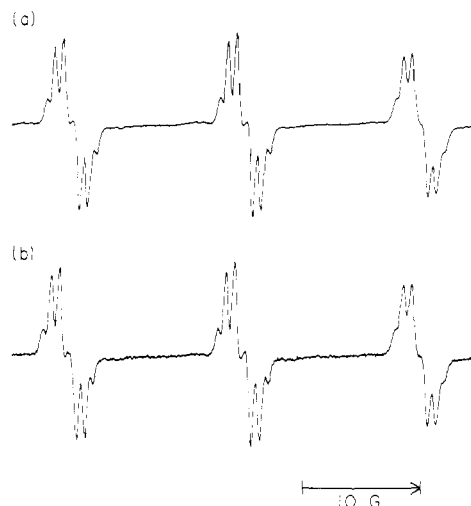


**Figure 7.** The ESR solution spectra of 3-doxyl-5 $\alpha$ -cholestane obtained (a) by extraction from the inclusion crystal and (b) directly from the recrystallized reaction product. In both cases the solvent was deoxygenated  $\text{CDCl}_3$  and the spectra were recorded at room temperature.

ing majority (>95%) of the recrystallized cholestane nitroxide is the equatorial isomer, 3(e)-doxyl-5 $\alpha$ -cholestane.<sup>17</sup>

**Acknowledgments.** We are pleased to acknowledge useful discussions with Dr. Shui Pong Van. This work was made possible by U. S. Public Health Service Grant CA 10337 from the National Cancer Institute. T.B.M. and O.H.G. gratefully acknowledge support from the National Institutes of Health Training Grant No. 2T01 GM00715-15 and Career Development Grant No. 1-K04 CA23359 from the National Cancer Institute, respectively.

#### References and Notes

- (1) J. F. W. Keana, S. B. Keana, and D. Beetham, *J. Amer. Chem. Soc.*, **89**, 3055 (1967).
- (2) L. J. Libertini, A. S. Waggoner, P. C. Jost, and O. H. Griffith, *Proc. Nat. Acad. Sci. U. S.*, **64**, 13 (1969).
- (3) W. L. Hubbell and H. M. McConnell, *Proc. Nat. Acad. Sci. U. S.*, **63**, 18 (1969).
- (4) J. Seelig, *J. Amer. Chem. Soc.*, **92**, 3881 (1970).
- (5) M. A. Hemminga and H. J. C. Berendsen, *J. Magn. Resonance*, **8**, 133 (1972).
- (6) R. D. Lapper, S. J. Paterson, and I. C. P. Smith, *Can. J. Biochem.*, **50**, 969 (1972).
- (7) E. Sackmann and H. Trauble, *J. Amer. Chem. Soc.*, **94**, 4482, 4492, 4499 (1972).
- (8) P. C. Jost and O. H. Griffith, *Arch. Biochem. Biophys.*, **159**, 70 (1973).
- (9) G. B. Birrell, S. P. Van, and O. H. Griffith, *J. Amer. Chem. Soc.*, **95**, 2451 (1973).
- (10) J. F. Brown, Jr., *Sci. Amer.*, **207** (1), 82 (1962).
- (11) H.-U. Lenné, *Acta Crystallogr.*, **7**, 1 (1954).
- (12) W. Schlenk, Jr., *Justus Liebigs Ann. Chem.*, **573**, 142 (1951).
- (13) N. Nicolaidis and F. Laves, *Z. Kristallogr., Kristallgeometrie, Kristallphys., Kristallchem.*, **121**, 283 (1965).
- (14) S. P. Van, G. B. Birrell, and O. H. Griffith, *J. Magn. Resonance*, **15**, 444 (1974).
- (15) P. Jost, L. J. Libertini, V. C. Hebert, and O. H. Griffith, *J. Mol. Biol.*, **59**, 77 (1971).
- (16) We have also achieved a partial purification of the axial isomer from the mother liquor and found its solution spectrum to be very different from that of the equatorial isomer. Due to lack of space these data will be presented elsewhere. Computer addition techniques show that as little as 20% axial isomer contamination markedly distorts the solution spectrum of the equatorial isomer and computer subtraction is sensitive enough to easily detect a 5% axial isomer contamination.
- (17) After this manuscript was submitted for publication, an article by Michon and Rassat appeared which also deals with this assignment of isomers [P. Michon and A. Rassat, *J. Org. Chem.*, **39**, 2121 (1974)]. It is interesting to note that these authors approached the problem from a quite different point of view. However, both studies are in agreement that the dominant isomer is 3(e)-doxyl-5 $\alpha$ -cholestane.